

## Dendronized Polymers with Peripheral Oligo(ethylene oxide) Chains: Thermoresponsive Behavior and Shape Anisotropy in Solution

Jérôme Roeser,<sup>†,‡,||</sup> Firmin Moingeon,<sup>†,⊥</sup> Benoît Heinrich,<sup>†</sup> Patrick Masson,<sup>†</sup> Françoise Arnaud-Neu,<sup>‡</sup> Michel Rawiso,<sup>§</sup> and Stéphane Méry<sup>\*†</sup>

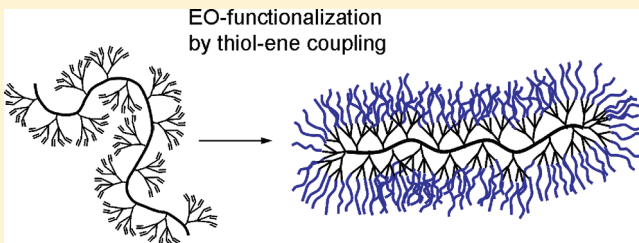
<sup>†</sup>Institut de Physique et Chimie des Matériaux de Strasbourg (IPCMS), Université de Strasbourg, CNRS UMR 7504, 23, rue du Loess, BP 43, 67034 Strasbourg cedex 02, France

<sup>‡</sup>Institut Pluridisciplinaire Hubert Curien (IPHC), Université de Strasbourg, CNRS UMR 7178, 25 rue Becquerel, 67087 Strasbourg cedex 02, France

<sup>§</sup>Institut Charles Sadron (ICS), UPR 22, CNRS, 23 rue du Loess, BP 84047, 67034 Strasbourg cedex 02, France

 Supporting Information

**ABSTRACT:** A series of dendronized polymers carrying oligo(ethyleneoxy) peripheral branches have been prepared by postpolymerization functionalization of multiallylic dendronized polymers using a radical addition of mercaptans, namely 2-methoxy(ethoxy)ethanethiol (EO2) and {2-(2-methoxyethoxy)ethoxy}ethanethiol (EO3). The functionalization proved to be quite efficient, leading to up to 6 or 9 EO chains per monomer repeating unit. A constant  $T_g$  value was observed independently of the material characteristics, indicating that  $T_g$  is ruled by the sole presence of EO chains. According to the hydrophilic and hydrophobic balance, some polymers exhibited a thermoresponsive behavior in water solution, characterized by a sharp lower critical solution temperature (LCST) transition and a small hysteresis. These LCST showed an unusual increase with DP, which might be correlated to a dilution effect and an increase of polymer hydrophilicity by densification of the dendritic coverage. By SAXS investigations and using a spherocylinder shape model, the polymers in solution (below the LCST) could be satisfactorily described. By increasing the DP, the shape of the macromolecule was found to evolve from a spherical to a spherocylinder shape with a constant cross section of ca. 40 Å.



### INTRODUCTION

Linear dendronized polymers are a particular class of branched polymers in which every repeating unit of a linear polymer carries a dendron.<sup>1</sup> Because of the presence of high chain density, the preparation of well-defined dendronized polymers remains a topical challenge. However, specific reactions and synthetic conditions have been reported to efficiently prepare dendronized polymers of high compactness via polymerization of dendritic macromonomers (macromonomer strategy)<sup>2</sup> or via grafting of dendrons, at once or stepwise, onto a preformed linear polymer backbone (grafting-onto or grafting-from strategy).<sup>3</sup>

The strong repulsive effect brought by sterically demanding dendrons is known to induce a stretching of the polymer backbone, possibly leading to (“core–shell”) cylindrical-shaped macromolecules.<sup>3a,4</sup> This shape anisotropy associated with polymer functionalization allows the preparation of a wide variety of functionalized “nanocylinders” leading to novel materials with specific properties.<sup>1,5</sup> Functional groups may be located at different levels of a dendronized polymer: the polymer backbone, the inner branches, or the dendron terminal branches. Functionalization of dendronized polymers is usually located at dendron termini, resulting in a surface-functionalized wormlike particle.

Kim and our group reported the preparation of allyl-covered dendronized polymers, having up to 9 allyl branches per monomer repeat unit,<sup>2h,3a,6</sup> by the grafting-from technique.<sup>3a,6</sup> More recently, we published an efficient preparation of allyl-ended dendronized polymers via the macromonomer route by using the anionic polymerization technique.<sup>2h</sup> We demonstrated that these multiallylic dendronized polymers constitute a versatile platform for the preparation of a large variety of surface-functionalized dendronized polymers.<sup>5</sup> Indeed, the peripheral allyl branches proved to be quite reactive toward radical addition of thiols, hydrosilylation, and hydroboration. Thus, it was possible to prepare jacketed polymers with oligo(ethylene oxide)s, perfluorinated chains, siloxane, or hydroxyl moieties.

Herein we describe the synthesis and characterization of dendronized polymers covered by oligo(ethylene oxide) (EO) chains, also referred as oligo(ethylene glycol) chains. These materials are prepared via a postpolymerization functionalization of multiallylic dendronized polymers, as mentioned above.<sup>5</sup> It has to be noted that other series of EO-based dendronized polymers

**Received:** July 21, 2011

**Revised:** September 26, 2011

**Published:** October 19, 2011

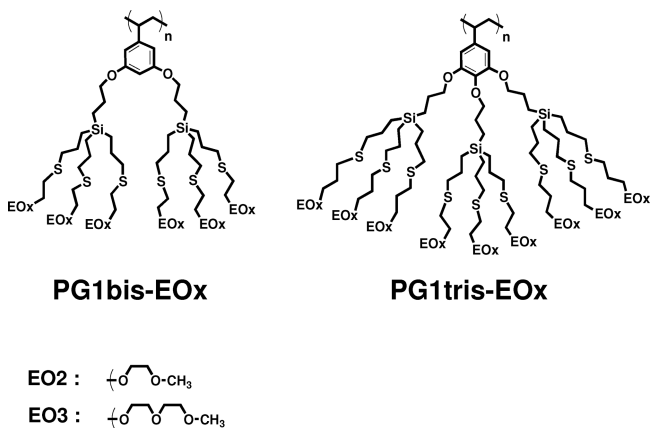


**Figure 1.** Molecular structure of the dendronized polymers with peripheral EO chains.

have been reported recently by Schlüter and Zhang et al.<sup>7</sup> However, their materials differ fundamentally from ours, from the preparation procedure, the chemical structure, and the location of the EO chains which are present at both the inner and peripheral parts of the dendrons. On the other hand, other structures of branched polymers having EO side chains have been reported in the literature but are classified as dendrimers,<sup>8</sup> poly(macromonomers),<sup>9</sup> or dendronized copolymers.<sup>10</sup>

The different series of EO-covered dendronized polymers presented in this report are shown in Figure 1. They correspond to bis-dendronized and tris-dendronized polymers of first generation. They are referred as PG1bis-EO<sub>x</sub> and PG1tris-EO<sub>x</sub> and contain respectively 6 and 9 EO end-chains per monomer repeat unit. The suffix *x* stands for the number of EO segments in the chains (*x* = 2 or 3).

At first sight and from a simple geometrical consideration, densely EO-functionalized polymers can be seen as wormlike objects made of a hydrophobic core wrapped with a hydrophilic EO mantle. These macromolecules are then expected to show singular behavior and properties that are intended to be presented and discussed here. The aim of the paper is to report results on the investigations of (i) the thermoresponse solubility in water with the influence of the polymers' characteristics, (ii) the polymers' thermal properties and the ability of the macromolecules to self-organize, and finally (iii) the structure and conformation of the polymers in solution.

## ■ EXPERIMENTAL SECTION

**Materials.** The starting multiallylic dendronized polymers PG1bis and PG1tris were prepared according to procedures already described.<sup>2h</sup> The mercaptan reagents 2-methoxy(ethoxy)ethanethiol (EO2) and {2-(2-methoxyethoxy)ethoxy}ethanethiol (EO3) were synthesized in three synthetic steps (60% overall yield) from the alcohol precursor, via the action of thiourea onto the tosylate intermediate as described in ref 11. Toluene was dried over KOH and distilled over sodium/benzophenone. AIBN was freshly recrystallized from MeOH before use. The SEC gel used to isolate the polymers from the reaction mixture was a SX1 Bio-Beads gel (Bio-Rad), given with a weight separation domain of 600–14 000 Da.

**Characterization and Studies.** <sup>1</sup>H (300 MHz) and <sup>13</sup>C (75 MHz) NMR spectra were measured using a Bruker AC300 spectrometer. Elemental analyses were carried out by the analytical department of the Institute Charles Sadron (ICS) in Strasbourg. Molecular weight determinations were performed at ICS by size exclusion chromatography

(SEC). For THF elution, the analysis was carried out on a Shimadzu chromatograph fitted with five PLGel 10  $\mu\text{m}$  Mixed B columns (styrene–divinylbenzene polymer gel) and by using three detection modes: a differential refractometer detector (Shimadzu RID-10A) calibrated with polystyrene standards, a UV detector ( $\lambda$  = 254 and 280 nm), and a multiangle laser light scattering (MALLS) detector (Wyatt TREOS,  $\lambda$  = 632.8 nm). For aqueous elution (0.1 M NaNO<sub>3</sub> and NaN<sub>3</sub>), the analyses were carried out on a DIONEX Ultimate 3000 chromatograph fitted with four Shodex OH-pack mixed columns (poly(hydroxy methacrylate)-based gel) and by using three detection modes: a differential refractometer OPTILAB REX from Wyatt Technol., a UV detector ( $\lambda$  = 254 and 280 nm), and a multiangle laser light scattering (MALLS) detector (Dawn Heleos from Wyatt Technol.). Molecular weight values ( $M_w$ ) were determined from direct  $d\eta/dc$  calculation, assuming 100% mass injected recovery. Differential scanning calorimetry (DSC) measurements were performed on a Q1000 equipment from TA Instruments equipped with a LNCS (liquid nitrogen cool system) cooling system in the temperature range from −150 to 50 °C, at a heating and cooling rate of 5 °C min<sup>−1</sup>. Measurements were performed on samples (3–8 mg) placed into 10  $\mu\text{L}$  aluminum pans under nitrogen. UV-vis transmission measurements for the determination of cloud points were carried out on a Uvikon XL spectrometer equipped with a thermoregulated bath using a Peltier system. The measurements were performed on polymer solutions (1–10 g L<sup>−1</sup>) in deionized water, placed into cuvettes of 1 mm path length. Transmittance (%) was recorded at 500 nm every minute at cooling and heating rates of 1 °C min<sup>−1</sup>. Small-angle neutrons scattering (SANS) experiments were conducted on the spectrometer PACE (Laboratoire Léon Brillouin, Saclay, France) by using 2.5 mm thick quartz cells and by setting the sample temperature at 10 ± 1 °C. Deuterated tetrahydrofuran (TDF) and water (D<sub>2</sub>O) were used as solvents. Data were formatted and calibrated with the PAxiNET software. Small-angle X-ray scattering (SAXS) measurements have been performed with the spectrometer D2AM (European Synchrotron Research Facility, Grenoble, France), by using sample holders with mica windows, the sample thickness being kept to 1 mm. Deionized water (H<sub>2</sub>O) was used as solvent. The sample temperature was controlled within 0.03 °C by using a home-built oven. Data treatment involved corrections for incident photon flux, sample transmission, sample thickness, intensity scattered from empty cell, and pure water. In this way the coherent scattered intensity  $I(q)$  was measured on an absolute scale according to the scattering vector  $q$  defined as  $q = 4\pi \sin(\theta/2)/\lambda$ , where  $\lambda$  is the wavelength of the incident beam and  $\theta$  the scattering angle. For SANS and SAXS sample preparation, polymer solutions at 2 wt % (and dilutions at 1 and 0.5 wt %) of the polymers in pure TDF, D<sub>2</sub>O, or H<sub>2</sub>O were prepared by sonication while maintaining the temperature below the LCST. The form factor of the particles is obtained from the coherent scattered intensity  $I(q)$  using an analogous procedure as previously described,<sup>2s</sup> provided the intermolecular correlations are neglected.

### General Procedure for Postpolymer EO Functionalization.

A dried tube was charged with previously prepared multiallylic dendronized polymers<sup>2h</sup> PG1bis or PG1tris (2 mmol of allyl branches), toluene (0.5 mL), the mercaptan EO2 or EO3 (4 mmol), and a solution of AIBN (7.9 mg, 2.7 mol %) in toluene (0.7 mL). After several freeze–pump–thaw cycles, the tube was sealed under vacuum and the mixture was stirred at 50 °C for 72 h. Isolation of the polymer from the unreacted mercaptan was then performed by passing the crude polymerization mixture through a column filled with a SEC gel and eluted by THF by gravity flow. The polymer fraction was concentrated and dried under vacuum at 50 °C to yield the EO-dendronized polymers (94–100% yield) as a transparent viscous oil. Typical data for some polymer representatives:

**PG1bis-EO2.** <sup>1</sup>H NMR (300 MHz, CDCl<sub>3</sub>)  $\delta$  ppm: 0.50–0.80 (br, 16H, SiCH<sub>2</sub>), 1.4–1.7 (br, 18H, CH<sub>2</sub> dendron and backbone), 1.7–1.9 (br, 1H, CH backbone), 2.55 (12H, CH<sub>2</sub>S), 2.7 (12H, CH<sub>2</sub>S), 3.35

(18H,  $\text{CH}_3\text{O}$ ), 3.5 (12H,  $\text{CH}_2\text{O}$ ), 3.6 (24H,  $\text{CH}_2\text{O}$ ), 3.9 (br, 4H,  $\text{CH}_2\text{OAr}$ ), 5.3–6.2 (br, 3H, aromatic).  $^{13}\text{C}$  NMR (75 MHz,  $\text{CDCl}_3$ )  $\delta$  ppm: 8.5 ( $\text{SiCH}_2$ ), 11.8 ( $\text{SiCH}_2$ ), 23.8 ( $\text{CH}_2$ ), 24.4 ( $\text{CH}_2$ ), 31.4 ( $\text{CH}_2\text{S}$ ), 36.3 ( $\text{CH}_2\text{S}$ ), 59.0 ( $\text{CH}_3\text{O}$ ), 70.1 ( $\text{CH}_2\text{O}$ ), 71.0 ( $\text{CH}_2\text{O}$ ), 71.9 ( $\text{CH}_2\text{O}$ ), 97.9 ( $\text{Ar}_4$ ), 107 ( $\text{Ar}_2$ ), 147 ( $\text{Ar}_1$ ), 159.9 ( $\text{Ar}_3$ ), signals from polymer backbone not detectable. Anal. Calcd (found) for  $(\text{C}_{62}\text{H}_{120}\text{O}_{14}\text{S}_6\text{Si}_2)_n$ : C, 55.65 (55.02); H, 9.04 (9.05); S, 14.38 (14.99); Si, 4.20 (4.51).

**PG1bis-EO3.**  $^1\text{H}$  NMR (300 MHz,  $\text{CDCl}_3$ )  $\delta$  ppm: 0.50–0.75 (br, 16H,  $\text{SiCH}_2$ ), 1.4–1.9 (br, 19H,  $\text{CH}_2$  and polymer backbone), 2.55 (12H,  $\text{CH}_2\text{S}$ ), 2.7 (12H,  $\text{CH}_2\text{S}$ ), 3.35 (s, 18H,  $\text{CH}_3\text{O}$ ), 3.55 (12H,  $\text{CH}_2\text{O}$ ), 3.7 (m, 48H,  $\text{CH}_2\text{O}$ ), 3.85 (br, 4H,  $\text{CH}_2\text{OAr}$ ), 5.3–6.2 (br, 3H aromatic).  $^{13}\text{C}$  NMR (75 MHz,  $\text{CDCl}_3$ )  $\delta$  ppm: 8.6 ( $\text{SiCH}_2$ ), 11.8 ( $\text{SiCH}_2$ ), 23.9 ( $\text{CH}_2$ ), 24.5 ( $\text{CH}_2$ ), 31.5 ( $\text{CH}_2\text{S}$ ), 36.4 ( $\text{CH}_2\text{S}$ ), 59.0 ( $\text{CH}_3\text{O}$ ), 70.2 ( $\text{CH}_2\text{O}$ ), 70.5 ( $\text{CH}_2\text{O}$ ), 70.6 ( $\text{CH}_2$ ), 71.0 ( $\text{CH}_2\text{O}$ ), 72.0 ( $\text{CH}_2\text{O}$ ), 97.9 ( $\text{Ar}_4$ ), 107 ( $\text{Ar}_2$ ), 146 ( $\text{Ar}_1$ ), 159.8 ( $\text{Ar}_3$ ), signals from polymer backbone not detectable. Anal. Calcd (found) for  $(\text{C}_{74}\text{H}_{144}\text{O}_{20}\text{S}_6\text{Si}_2)_n$ : C, 55.46 (55.51); H, 9.06 (9.14); S, 12.01 (11.84); Si, 3.51 (3.70).

**PG1tris-EO2.**  $^1\text{H}$  NMR (300 MHz,  $\text{CDCl}_3$ )  $\delta$  ppm: 0.50–0.70 (br, 24H,  $\text{SiCH}_2$ ), 1.4–1.9 (br, 27H,  $\text{CH}_2$  and polymer backbone), 2.55 (m, 18H,  $\text{CH}_2\text{S}$ ), 2.7 (m, 18H,  $\text{CH}_2\text{S}$ ), 3.37 (s, 27H,  $\text{CH}_3\text{O}$ ), 3.54 (18H,  $\text{CH}_2\text{O}$ ), 3.62 (m, 36H,  $\text{CH}_2\text{O}$ ), 3.77 (4H,  $\text{CH}_2\text{OAr}$ ), 3.90 (2H,  $\text{CH}_2\text{OAr}$ ), 6.1 (br, 2H aromatic).  $^{13}\text{C}$  NMR (75 MHz,  $\text{CDCl}_3$ )  $\delta$  ppm: 8.8 ( $\text{SiCH}_2$ ), 11.9 ( $\text{SiCH}_2$ ), 17.7 ( $\text{CH}_2$ ), 24.5 ( $\text{CH}_2$ ), 31.5 ( $\text{CH}_2\text{S}$ ), 36.4 ( $\text{CH}_2\text{S}$ ), 59.0 ( $\text{CH}_3\text{O}$ ), 70.2 ( $\text{CH}_2\text{O}$ ), 71.0 ( $\text{CH}_2\text{O}$ ), 71.9 ( $\text{CH}_2\text{O}$ ), 153 ( $\text{Ar}_3$ ), signals from other aromatics and from polymer backbone not detectable. Anal. Calcd (found) for  $(\text{C}_{89}\text{H}_{176}\text{O}_{21}\text{S}_9\text{Si}_3)_n$ : C, 54.33 (54.51); H, 9.32 (9.14); S, 14.76 (14.85); Si, 4.31 (4.53).

**PG1tris-EO3.**  $^1\text{H}$  NMR (300 MHz,  $\text{CDCl}_3$ )  $\delta$  ppm: 0.50–0.75 (br, 24H,  $\text{SiCH}_2$ ), 1.4–1.9 (br, 27H,  $\text{CH}_2$  and polymer backbone), 2.55 (m, 18H,  $\text{CH}_2\text{S}$ ), 2.7 (m, 18H,  $\text{CH}_2\text{S}$ ), 3.35 (s, 27H,  $\text{CH}_3\text{O}$ ), 3.55 (18H,  $\text{CH}_2\text{O}$ ), 3.7 (72H,  $\text{CH}_2\text{O}$ ), 3.8 (4H,  $\text{CH}_2\text{OAr}$ ), 3.9 (2H,  $\text{CH}_2\text{OAr}$ ), 6.1 (br, 2H aromatic).  $^{13}\text{C}$  NMR (75 MHz,  $\text{CDCl}_3$ )  $\delta$  ppm: 8.9 ( $\text{SiCH}_2$ ), 11.9 ( $\text{SiCH}_2$ ), 17.7 ( $\text{CH}_2$ ), 24.5 ( $\text{CH}_2$ ), 31.6 ( $\text{CH}_2\text{S}$ ), 36.4 ( $\text{CH}_2\text{S}$ ), 59.0 ( $\text{CH}_3\text{O}$ ), 70.2 ( $\text{CH}_2\text{O}$ ), 70.5 ( $\text{CH}_2\text{O}$ ), 70.6 ( $\text{CH}_2\text{O}$ ), 71.0 ( $\text{CH}_2\text{O}$ ), 72.0 ( $\text{CH}_2\text{O}$ ), 153 ( $\text{Ar}_3$ ), signals from other aromatics and from polymer backbone not detectable. Anal. Calcd (found) for  $(\text{C}_{107}\text{H}_{212}\text{O}_{30}\text{S}_9\text{Si}_3)_n$ : C, 54.65 (54.51); H, 9.09 (9.06); S, 12.27 (12.53); Si, 3.58 (3.70).

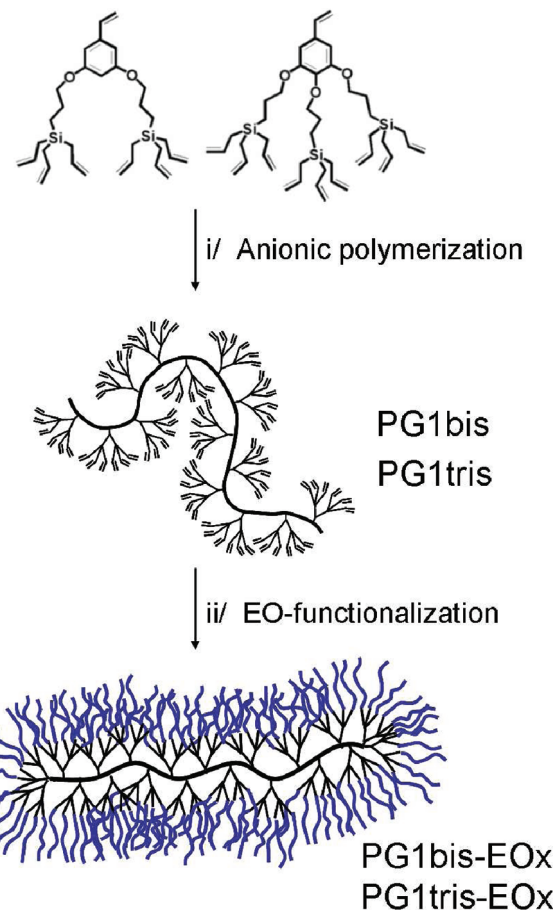
## ■ RESULTS AND DISCUSSION

**Synthesis and Characterization.** The synthesis of the dendronized polymers followed typical procedures already described in previous reports. The dendronized polymers carrying EO side chains (PG1bis-EOx and PG1tris-EOx) were synthesized in two steps, i.e., anionic polymerization of multiallylic dendronized macromonomers to produce the polymers PG1bis and PG1tris,<sup>2h</sup> followed by grafting of the EO side chains by thiol–ene coupling<sup>5</sup> (Scheme 1).

As already reported,<sup>2h</sup> the anionic polymerization of the allyl-ended dendritic macromonomers is fast in the oligomer regime, leading to polymers with a monomodal and symmetrical molecular weight distribution, associated with a narrow polydispersity. For higher degree of polymerization (DP > 30 for the bis-dendronized PG1bis), the polymer growth is considerably reduced and competes with transfer reaction (mostly intramolecular), leading to a slight increase of polydispersity (PDI > 1.3). In the case of the bulkier tris-dendronized macromonomer, the propagation proceeds very slowly from the beginning and could only lead to oligomers of PG1tris.

Different bis-dendronized PG1bis (DP = 12, 26, 56, and 82) and tris-dendronized polymers PG1tris (DP = 6) of first

**Scheme 1.** Two-Step Preparation Procedure of EO-Functionalized Dendronized Polymers PG1bis-EOx and PG1tris-EOx by (i) Anionic Polymerization of Allyl-Ended Dendritic Macromonomers, Followed by (ii) Thiol–Ene Coupling with Short EO Chains



generation were prepared in this way. They were further used for the functionalization step by using two different short EO chains having respectively 2 and 3 EO segments.<sup>5</sup> The resulting polymers, PG1bis-EOx and PG1tris-EOx, allowed us to study the effect of the molecular weight, the chain density, and the EO content on the properties of the materials. The functionalization procedure was adapted from Lorenz et al.'s<sup>12</sup> and optimized by a short study of grafting efficiency on monomer analogues in order to avoid the well-known cyclization side reaction.<sup>13</sup> Quantitative functionalization without detectable side reaction could be obtained by varying the experimental conditions (time, temperature, and concentration), and these optimized conditions were applied for polymer functionalization. Azobis(isobutyronitrile) (AIBN) was chosen as the radical source, and a 2-fold excess of the mercaptan with respect to double bonds was applied. Functionalization reactions were then carried out for 72 h in toluene in sealed tubes after several freeze–pump–thaw cycles. The functionalized polymers were obtained in quantitative yield as transparent viscous oils after simple removal of the unreacted mercaptans by size exclusion chromatography (eluted by THF). The resulting polymers are highly soluble in conventional organic solvents such as THF, diethyl ether, cyclohexane, dichloromethane, and for some of them in water (vide infra).

**Table 1. Functionalization of the Multiallylic Dendronized Polymers by EO Chains**

	starting multiallylic polymers <sup>a</sup>			EO functionalization <sup>a</sup>			
	$M_w^a$ (Da)	PDI <sup>b</sup>	DP <sub>n</sub> <sup>c</sup>	chain dn/dc	$M_w^a$ (Da)	PDI <sup>b</sup>	% grafting <sup>d</sup>
PG1bis	6 600	1.05	12	EO2 0.118	16 600	1.12	99
				EO3 0.108	20 500	1.10	99
	15 500	1.14	26	EO2 0.120	35 000	1.20	98
				EO3 0.110	44 500	1.16	98
PG1tris	47 400	1.63	56	EO2 0.120	155 600	1.82	96
				EO3 0.110	244 300	1.78	98
	80 600	1.89	82	EO2 0.120	482 000	2.60	98
				EO3 0.100 <sup>e</sup>	443 000 <sup>e</sup>	1.90 <sup>e</sup>	98
PG1tris	5 030	1.07	6	EO2 0.119	12 800	1.08	98
				EO3 0.116	16 200	1.20	98

<sup>a</sup> Determined from SEC analysis in THF using MALLS detection.  
<sup>b</sup> Polydispersity determined by SEC using refractive index detection from polystyrene standard calibration.  
<sup>c</sup> Number-average degree of polymerization calculated from  $M_w$  and PDI.  
<sup>d</sup> Functionalization yield determined from <sup>1</sup>H NMR ( $\pm 2\%$ ).  
<sup>e</sup> Underestimated values obtained from SEC analysis in water (see Supporting Information).

The characteristics of the polymers before and after modification are reported in Table 1. As indicated by SEC (Figure 2), the starting multiallylic dendronized polymers PG1bis show a monomodal and narrow molecular weight distribution for low DPs (PDI < 1.2 for DP = 12 and 26) that broadens at higher DPs (PDI  $\sim$  1.6–1.9 for DP = 56 and 82). From the comparison of the SEC peaks for polymers PG1bis-EO2 and PG1bis-EO3 with PG1bis, one can clearly notice the increase of molecular weights without significant change in the shape of the molecular weight distributions, suggesting that no major side reactions occur during the functionalization step (Figure 2). The same observations can be made for the tris-dendronized polymers (Figure 3). As shown in Table 1, constant dn/dc values are obtained within the two series of polymers PG1bis-EO2 and PG1bis-EO3, indicating that the polymers have the same molecular architecture and composition. One representative polymer (PG1bis-EO3 of DP = 82), however, shows a lower dn/dc value. In this specific case, the SEC analysis could not be performed in THF because of aggregation issues. Performed in water, the analysis led to underestimated values due to specific affinity of the polymer for the stationary phase of the SEC column (see Experimental Section).

FT-IR analysis showed the characteristic ether band ( $\tilde{\nu} = 1100 \text{ cm}^{-1}$ ) whereas no C=C stretching band ( $\tilde{\nu} = 1650 \text{ cm}^{-1}$ ) was noticeable anymore, suggesting the complete conversion of allyl branches into EO-thioether moieties.<sup>5</sup> This observation was confirmed by <sup>1</sup>H NMR. The spectra clearly show the characteristic signals of protons of the grafted (thio)ether chains at  $\delta = 3.3$ –3.8 ppm ( $\text{CH}_2\text{O}$ ) and 2.4–2.8 ppm ( $\text{CH}_2\text{S}$ ). Only a careful examination of the NMR spectra could reveal for some polymers a residual amount of unreacted allyl branches at  $\delta = 5.7$  and 4.8 ppm ( $\text{CH}=\text{CH}_2$ ). This was the case, for instance, for the bulky PG1tris-EO3 (Figure 4). The <sup>1</sup>H and <sup>13</sup>C NMR spectra for all compounds are given in the Supporting Information. The quantification of the remaining allyl branches from <sup>1</sup>H NMR analysis was used to determine the grafting yield of the functionalization. The results listed in Table 1 bring evidence of a quasi-complete functionalization leading to grafting yield values over 96% for all polymers. These results demonstrate the

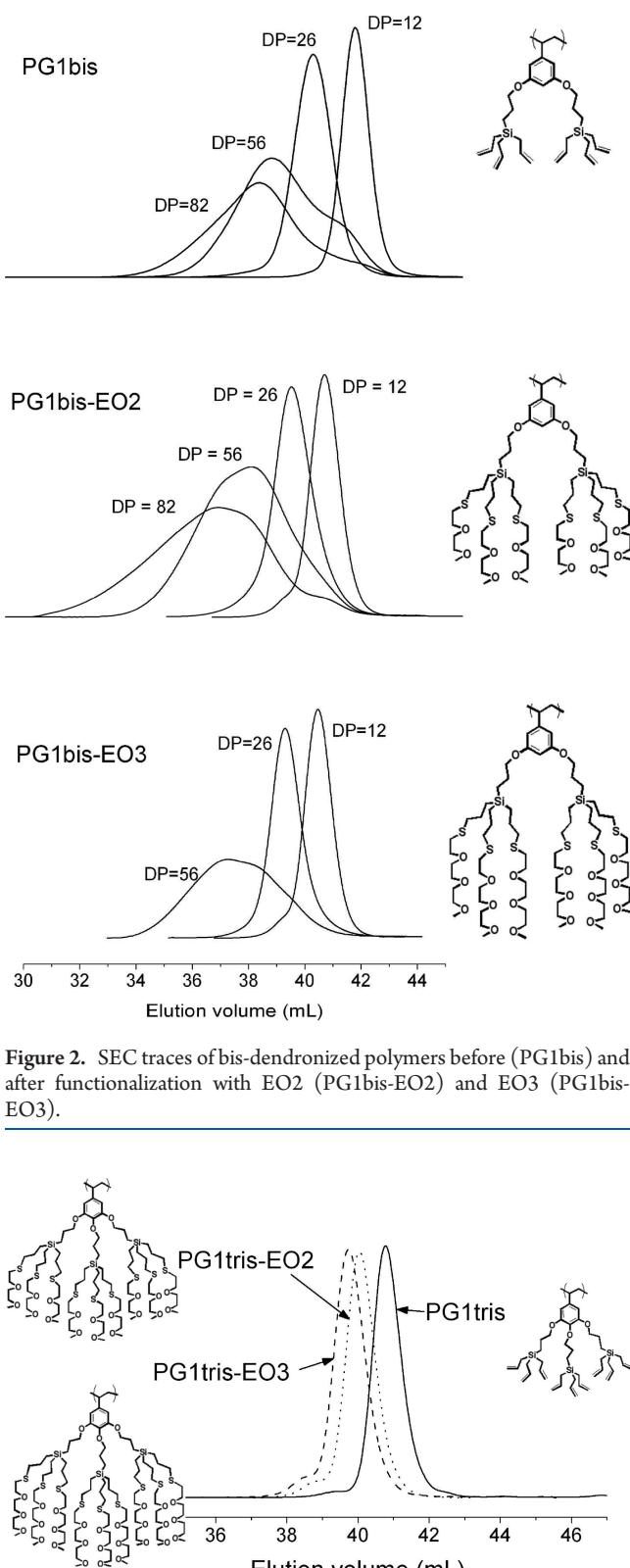


**Figure 2.** SEC traces of bis-dendronized polymers before (PG1bis) and after functionalization with EO2 (PG1bis-EO2) and EO3 (PG1bis-EO3).

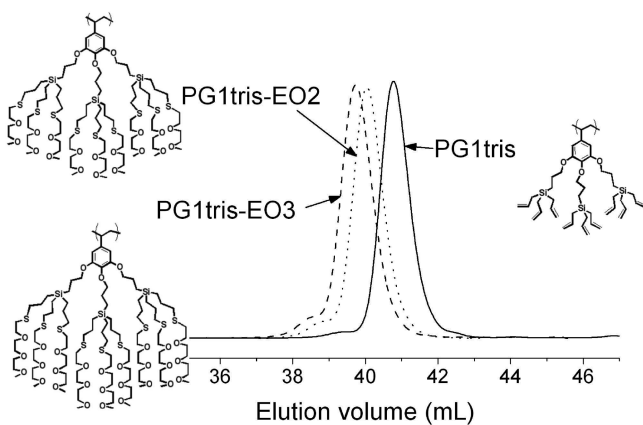


**Figure 3.** SEC traces of tris-dendronized polymers before (PG1tris) and after functionalization with EO2 (PG1tris-EO2) and EO3 (PG1tris-EO3).

remarkable efficiency of the radical addition of thiols to functionalize bulky multiallylic polymers with EO chains.

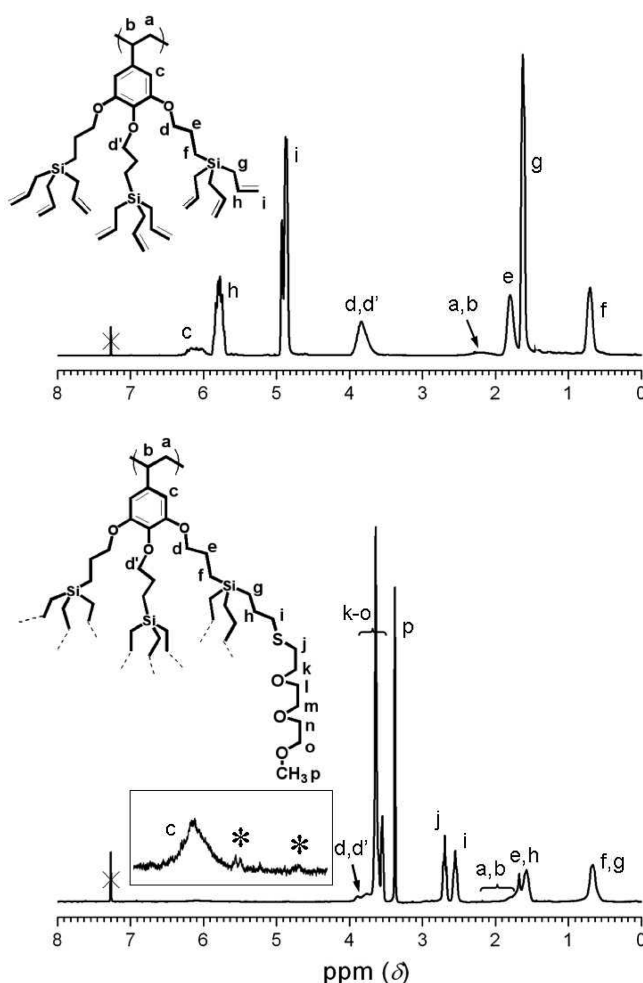


**Figure 4.** <sup>1</sup>H NMR spectra of tris-dendronized polymers, before (PG1tris) and after (PG1tris-EO3) functionalization with EO chains. Quasi-quantitative functionalization can be deduced from the traces of residual allyl branches, indicated by an asterisk in the enlarged section.

Finally, the “macromonomer” strategy was attempted to prepare the polymer PG1bis-EO3, via the direct radical polymerization of the corresponding styrene macromonomer containing the EO branches (see Supporting Information). However, this approach revealed to be unsuccessful for our macromonomer, as evidenced by the presence of aggregates in the reaction products. The lack of control of the polymerization was likely due to cross-linking reactions.

**Thermal Bulk Properties.** All functional dendronized polymers exhibit a purely amorphous character. A glass transition temperature ( $T_g$ ) is observed by DSC at very low temperatures, ca.  $-80^\circ\text{C}$ . Comparably low  $T_g$  values have already been reported for other dendronized polymers having pendant OE chains.<sup>7a</sup> Very surprisingly, however, and as observed in Figures 5 and 6, the  $T_g$  value of our polymers does not depend on the material characteristics: DP, side chain density (PG1bis-EO or PG1tris-EO), and EO chain length (EO2 or EO3). This behavior is different from the multialylic dendronized polymers, which show a  $T_g$  increase with DP in the oligomer regime, to level off at higher DP (Figure 5). Furthermore, and in the same way, the functional macromonomers (G1bis-EO2, G1bis-EO3, and G1tris-EO3) exhibit also a similar  $T_g$  value at about  $-80^\circ\text{C}$  (Figure 6). Thus,

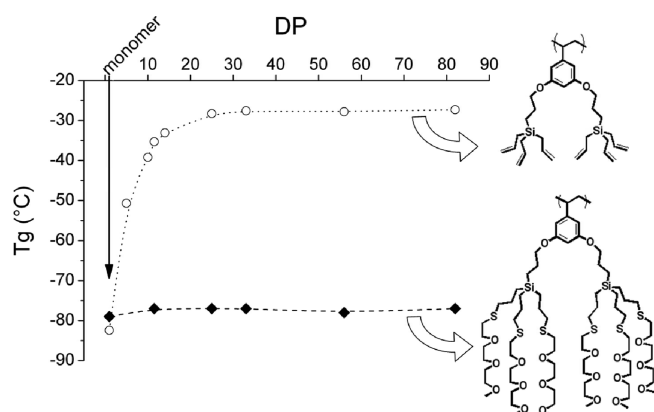


**Figure 5.** Variation of  $T_g$  values with DP for P(G1bis-EO3) and its multialylic polymer precursor. Values for macromonomers G1bis and G1bis-EO3 are also reported.

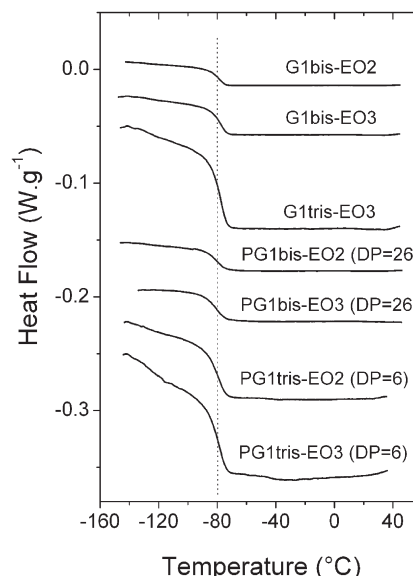


**Figure 6.** DSC endotherms showing similar  $T_g$  values for all EO-based dendronized macromonomers (G1bis-EO2, G1bis-EO3, G1tris-EO3) and polymers (PG1bis-EO2, PG1bis-EO3, PG1tris-EO2, PG1tris-EO3).

the sole presence of EO chains, whatever their content or material type, is enough to produce a definite  $T_g$  value in the temperature range between  $-77$  and  $-80^\circ\text{C}$ . No additional  $T_g$  value, possibly related to the polymer backbone, could be detected in EO-functionalized polymers despite fine calorimetric analyses.

The lack of supplementary heat signal in DSC analysis suggests that no liquid crystal phase transition is present in the bulk materials. Absence of thermotropic mesophase was further confirmed from the lack of birefringence as checked by polarizing optical microscopy. Such organization could possibly arise from microphase separation effects, as already observed for analogous functionalized polymers with perfluorinated chains or siloxane moieties.<sup>5</sup> Investigations of lyotropic organization in concentrated aqueous solutions (up to 95 wt % polymer in water) also revealed to be unsuccessful. Finally, TGA measurements showed that all EO-functionalized polymers are thermally stable under air until  $200^\circ\text{C}$ , before significant weight loss was observed.

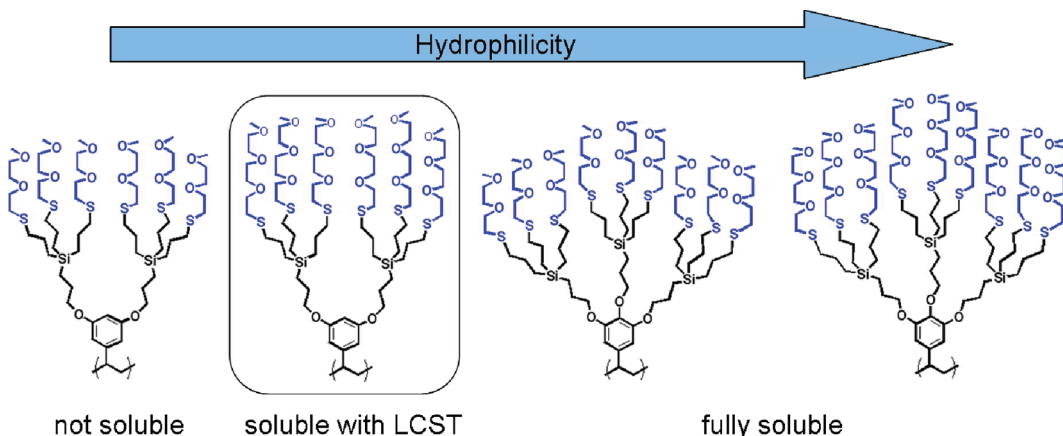


**Figure 7.** Evolution of hydrophilicity and water solubility for EO-dendronized polymers as a function of chain density (PG1bis-EOx or PG1tris-EOx) and EO chain length (EO2 or EO3).

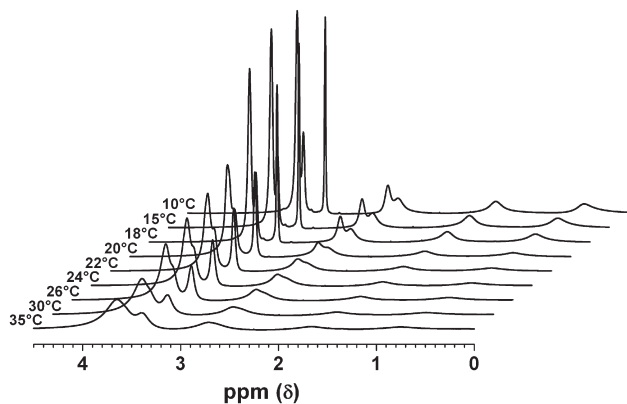


**Figure 8.**  $^1\text{H}$  NMR spectra of PG1bis-EO3 of DP = 12 recorded from 10 to 35  $^\circ\text{C}$  in  $\text{D}_2\text{O}$  ( $3 \text{ g L}^{-1}$ ).

**Thermoresponsive Properties in Water.** The balance between the hydrophobic and the hydrophilic part of the polymers can be finely tuned by modifying the density and the length of the grafted EO chains. Indeed, in our case the hydrophilicity of the polymers can be increased by adjusting both chain length and chain density as can be seen on Figure 7. The tris-dendronized polymers having the highest density of EO chains (PG1tris-EO2 and PG1tris-EO3) are fully soluble in water. On the opposite, the bis-dendronized polymers bearing the shortest EO chains (PG1bis-EO2) are not water-soluble. In between, the bis-dendronized polymers with longer chain length (PG1bis-EO3) exhibit a lower critical solution temperature (LCST) in water.

LCST is known to arise from a subtle balance between hydrophilic and hydrophobic interactions.<sup>14</sup> While at low temperature the hydrophilic part is able to counterbalance the unfavorable hydrophobic interactions and allow solubilization, a weakening of the hydrogen bonds provided by a temperature increase is enough to induce a sudden dehydration of the polymer leading to its brutal aggregation. This phenomenon is fully reversible and may find many applications in “smart materials” for biomedicine, for instance.<sup>9d,15</sup> The presence of LCST is well-known for the reference polymer poly(*N*-isopropylacrylamide) (PNIPAAm),<sup>16</sup> but it has also been described in some EO-branched polymers,<sup>17</sup> including dendrimers<sup>8,18</sup> and dendronized polymers.<sup>7b–f</sup> Thermoresponsive

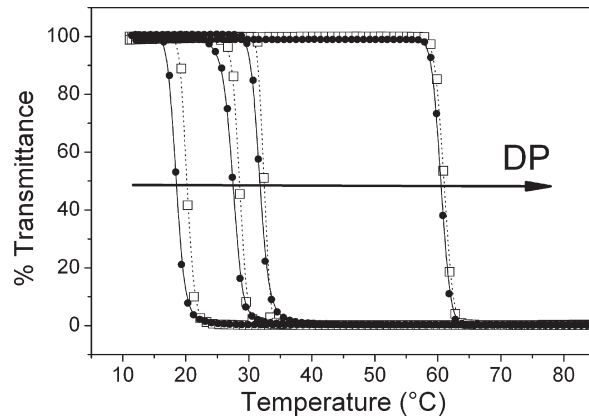


**Figure 9.** Plots of transmittance versus temperature for aqueous solution ( $3 \text{ g L}^{-1}$ ) of PG1bis-EO3 of different DP values (DP = 12, 26, 56, and 82), recorded at 500 nm at a rate of  $1 \text{ }^\circ\text{C min}^{-1}$  [heating ( $\square$ ) and cooling ( $\bullet$ ) runs].

behavior has also been reported in dendrimers<sup>19</sup> and dendronized polymers free from EO chains.<sup>20</sup>

The LCST could be first evidenced by variable temperature  $^1\text{H}$  NMR spectroscopy in  $\text{D}_2\text{O}$ . The collapse of the dendritic EO side chains can be clearly visualized by the decrease of peak intensity and the broadening of signals, due to a diminution of chain mobility. Take polymer PG1bis-EO3 of DP = 12 for instance; the change in the  $^1\text{H}$  NMR signals is observed at temperatures above 18  $^\circ\text{C}$ , as can be seen in Figure 8. A more convenient method to characterize the demixing/solubilization process lays on the cloud point detection ( $T_{\text{cloud}}$ ) method which consists of monitoring the optical transmission as a function of temperature. Turbidity measurements were done with aqueous solutions of polymers PG1bisOE3 ( $3 \text{ g L}^{-1}$ ) of different DP values. The plots of transmittance versus temperature are shown in Figure 9.

The temperature dependence of the transmittance (Figure 9) shows comparable features to other previously reported thermo-responsive EO-branched polymers.<sup>7b–e,17</sup> The thermal transition is observed in both heating and cooling processes with the whole event taking place within a few degrees, less than 8  $^\circ\text{C}$  (Table 2). This transition is also characterized by a narrow hysteresis between the heating and cooling processes, typically

**Table 2.**  $T_{\text{cloud}}$  Values and Phase Transition Broadness as a Function of DP and Molar Concentration of PG1bis-EO3

DP	wt conc (g L <sup>-1</sup> )	molar conc (mmol L <sup>-1</sup> )	$\Delta T$ global (°C)	$\Delta T$ hysteresis (°C)	$T_{\text{cloud}}$ (°C)
12	3	0.154	8	2	21
26	3	0.072	8	1.5	28
56	3	0.033	7	1	32
82	3	0.023	6	0.5	61

less than 2 °C, and as low as 0.5 °C for polymers of higher DP values. Such sharp transition ( $\Delta T < 8$  °C) and narrow hysteresis ( $\Delta T < 2$  °C) seem to be a common feature of well-defined EO-branched thermosensitive macromolecules.<sup>7b–e,17c,18</sup>

A more striking result is the strong dependence of the cloud point with DP (Figure 9). This behavior is uncommon since LCST is described to be relatively unaffected by DP, although a strong influence of the molecular weight has been found in dendrimers of globular shape.<sup>19</sup> Furthermore, if a slight dependence with DP is detected, the opposite effect is usually observed (i.e., a decrease of  $T_{\text{cloud}}$  by increasing DP) because of the reduced entropy of mixing.<sup>7c,17a–17c</sup> The trend may be reversed, especially at low DP, if the degree of hydrophilicity is found to increase with DP,<sup>17d,21,22</sup> as it seems to be the case in our polymers. Our polymers carry sterically demanding dendritic side groups, terminated by hydrophilic EO units. At very low DPs, the side groups should get enough space to move, especially at polymer ends, making accessible all (hydrophobic and hydrophilic) parts of the macromolecule to water molecules. At higher DPs, however, a densification of the side groups is expected, leading to the formation of a more compact EO-shell that should increasingly mask the hydrophobic inner core of the macromolecule. In overall, the apparent hydrophilic character of the polymers should increase with DP by congestion effect, resulting in an increase of  $T_{\text{cloud}}$ .

Another explanation for the increase of  $T_{\text{cloud}}$  with DP may be related to a dilution effect, especially in the oligomer regime. For the same mass concentration, a higher DP results in a lower molar concentration, i.e., a dilution of macromolecules, which is known to strongly influence  $T_{\text{cloud}}$ .<sup>23</sup> In our case, solutions (3 g L<sup>-1</sup>) of polymers of increasing DP from 12 to 82 corresponds to a decrease of the molar concentration of the macromolecules from 0.154 to 0.023 mmol L<sup>-1</sup> (Table 2). Further confirmation of the concentration dependence on demixing temperature is demonstrated by the plot given in Figure 10, showing the variation of  $T_{\text{cloud}}$  for the polymer PG1bis-EO3 (DP = 56) in the concentration range 1–10 g L<sup>-1</sup> (i.e., 0.011–0.111 mmol L<sup>-1</sup>). All these results indicate that the observed increase of  $T_{\text{cloud}}$  with DP should probably result from at least two concomitant factors, namely a polymer dilution effect and an increase of polymer hydrophilicity (due to a densification of the dendritic coverage).

To conclude with thermosensitivity and unlike other thermo-responsive EO-branched polymers,<sup>7b,17d</sup> our polymer PG1bis-EO3 was found to be only weakly thermally sensitive to addition of sodium ions (Na<sup>+</sup>), bringing evidence of absence of affinity of the EO end-branches of the dendritic side groups to Na<sup>+</sup>. A completely different behavior was observed with silver ions (Ag<sup>+</sup>) which led to a drastic increase of  $T_{\text{cloud}}$  with addition of a minor amount of Ag<sup>+</sup>, due to a high and selective affinity of the EO dendritic side groups with Ag<sup>+</sup>. Complexation properties of our EO-based dendronized polymers with cations, and Ag<sup>+</sup> in particular, will be intensively described in a subsequent paper.

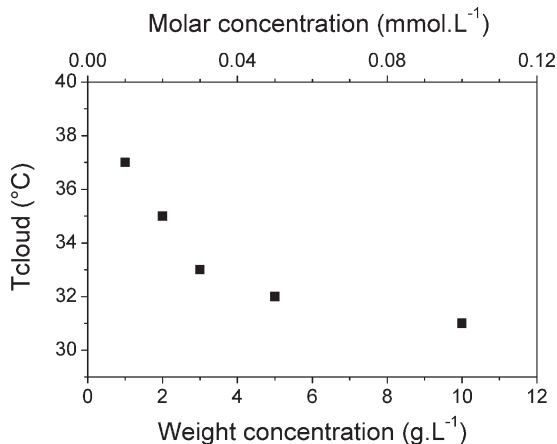


**Figure 10.** Evolution of  $T_{\text{cloud}}$  of polymer PG1bis-EO3 of DP = 56 as a function of both weight (g L<sup>-1</sup>) and molar (mmol L<sup>-1</sup>) concentration in water.

**Structural Properties in Solution.** One may easily imagine that conformation and morphology of isolated EO-based dendronized polymers in solution are affected by the solvent type (water versus organic one) and by the DP of the polymers. SANS and SAXS techniques are powerful techniques to investigate the structural properties of complex molecular structures, such as dendronized polymers.<sup>2f,3a,4a–4d</sup> In this work, both techniques have been used and led to the same results. In general, the SANS technique was preferred because of its accuracy, especially at lower scattering vectors. All studies were performed on the PG1bis-EO3 polymers of different molecular weights (DP = 12, 24, and 56) in solution in water and tetrahydrofuran. Analyses were performed at 10 °C (i.e., well below the LCST). However, a structural characterization was performed by SAXS at temperatures near the LCST, as described below.

At first, structural changes were investigated by SAXS in proximity to LCST for one representative polymer (PG1bis-EO3, DP = 24). The results do not show any structural change at low temperatures prior to the transition. As deduced from plots in Figure 11, no significant change is observed in the scattering curves in the intermediate (Figure 11a) and the Porod  $q$ -regions (Figure 11b). Beyond the LCST, however, a drastic change of the scattering curves is observed (i.e., a collapse of scattering intensity in the intermediate region and a shift of the position of the first maximum to higher  $q$  values in the Porod region) which is difficult to analyze since the transition is associated with phase separation and precipitation (Figure 11). The absence of observable structural change at the LCST might be explained by the too large temperature gaps explored. As a matter of fact, by using dynamic light scattering and cryo-TEM experiments, Schlüter and Zhang et al. could bring evidence of a progressive shrinking of their EO-based dendronized polymers prior to LCST, leading to the formation of well-defined and rather stable spherical-shaped mesoglobules.<sup>7e</sup> In other dendronized polymers, Gao et al. could visualize large and uniform spherical aggregates by optical microscopy.<sup>20b</sup>

Next are the results obtained by SAXS on the polymer series in both solvents: deuterated tetrahydrofuran (TDF) and deuterated water (D<sub>2</sub>O). The form factors recorded for the three polymers PG1bis-EO3 (DP = 12, 24, and 56) in TDF are shown in Figure 12. As immediately noticed, the curves superimpose on each other at high scattering vectors ( $q$ ) but move away from

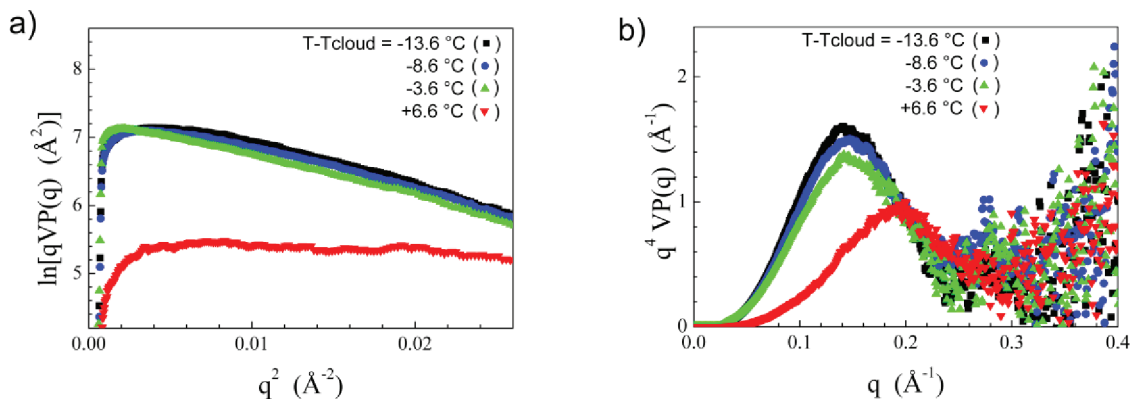


**Figure 11.** Form factors in the intermediate regions (a) and in the Porod representation (b), determined by SAXS for aqueous solutions of PG1bis-EO3 (DP = 24, 1 wt % in  $\text{H}_2\text{O}$ ) at different  $T - T_{\text{cloud}}$  values.

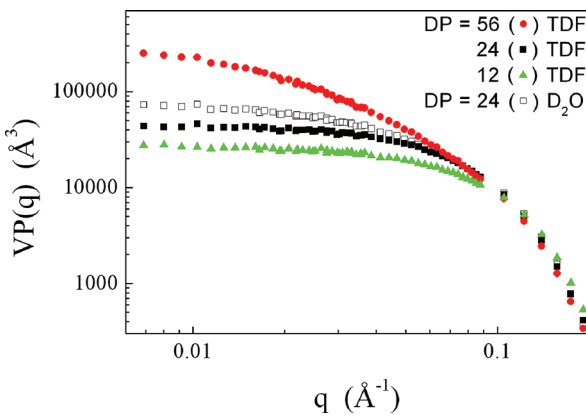


**Figure 12.** Form factors determined by SANS from TDF and  $\text{D}_2\text{O}$  solutions of polymers PG1bis-EO3 as a function of DP.

each other at small  $q$  values. The latter behavior is the trivial consequence of the increase of polymer chain length, while the former behavior indicates that the general shape of the polymer does not change much within the series. The substitution of TDF solvent for  $\text{D}_2\text{O}$  does not modify significantly the general shape of the scattering curve, as similar form factors are determined at large  $q$  values for solutions of the same polymer (DP = 24) in both solvents (also displayed in Figure 12). At small  $q$  values, however, a marked separation of the two curves is observed, which is found to further increase with polymer concentration and that most probably indicates the presence of aggregates in aqueous solution.

This last section is dedicated to the morphology of isolated polymers in solution. Because of the architecture of the EO-dendronized polymers and the dense EO coverage, it is expected that the shape of the scattering objects is close to a cylinder.<sup>5</sup> In addition, different shapes of cylinder tips can be imagined,<sup>24</sup> but the simplest model, consisting of hemispherical terminations (i.e., the spherocylinder model), is the one considered here.

The mean diameter of the cylinders can be deduced from the linear decrease of the cross-section term in the Guinier representation: about 40 Å for polymers of DP = 56 and 24 and about 37 Å for polymer of DP = 12 (Figure 13a). Since the molecular volume is known from dilatometric measurements,<sup>5</sup> the spherocylinder geometry is entirely determined by the section. As a result, the two former polymers can be schematized as spherocylinders with

aspect ratios of 3 and 1.5 (DP = 56 and 24, respectively), while the spherocylinder model of the latter gives an aspect ratio of about 1.0 (DP = 12) and can therefore be assimilated to a sphere (Figure 14). This shape evolution within the series corresponds to an increase of  $S/V$  (cross section over volume) ratios which is consistent with the shifts between scattering curves in the Porod representation (Figure 13b). Despite the deviation of the curves at highest  $q$  values (due to low signals and errors in the subtraction of the incoherent scattering contribution), the general aspect of the curves suggests a superimposition of the oscillation term on the Porod plateau that indicates the existence of macromolecular objects with sharp interfaces. The coordinates of this plateau is found to be in good agreement with the  $2\pi S/V$  values calculated from the spherocylinder model, i.e., 0.71, 0.81, and 0.94 Å<sup>-1</sup> for the three polymer series (DP = 56, 24, and 12, respectively).

Actually, since the last polymer of the series (DP = 12) is supposed to have a quasi-spherical shape, the oscillations' minima and maxima might be considered as sphere oscillations. Thus, analyses of the oscillations using a sphere model lead to a sphere diameter of 39 Å, which is in good agreement with the value previously calculated from the molecular volume (37 Å) and which also corresponds to the spherocylinder diameter value ( $d$ ) of polymers of higher DPs ( $d = 40$  Å). Another set of calculations involves the polymer of highest aspect ratio (DP = 56) for which a  $q^{-1}$  decay domain associated with the cylinder length is expected.<sup>25</sup> Indeed, the Holzer representation for this polymer contains such a characteristic plateau (Figure 15a). The  $q$  range of this plateau is compatible with the model aspect ratio, but the ordinate fits longer cylinders (150 Å vs 120 Å). The difference is attributed to a relatively large polydispersity (PDI = 1.9, see Table 1), i.e., a wide distribution of the polymer lengths, since the fractions of longer polymer chains naturally overestimate the calculated cylinder length value. It should be emphasized that the lengths determined from the volume over cross-section ratios are more realistic, as the polymer length and therefore the polydispersity have no influence on the cross section.

Finally, the Guinier domain could not be reached for polymer of DP = 56 because of the large size of the scattering objects and the relatively large polydispersity (Figure 15b). As a matter of fact, near the low angle limit, the form factor exhibits an upward deviation which is not related to aggregation or other intermolecular contribution since the curve remains unchanged when concentration is varied. Again, this deviation most likely results

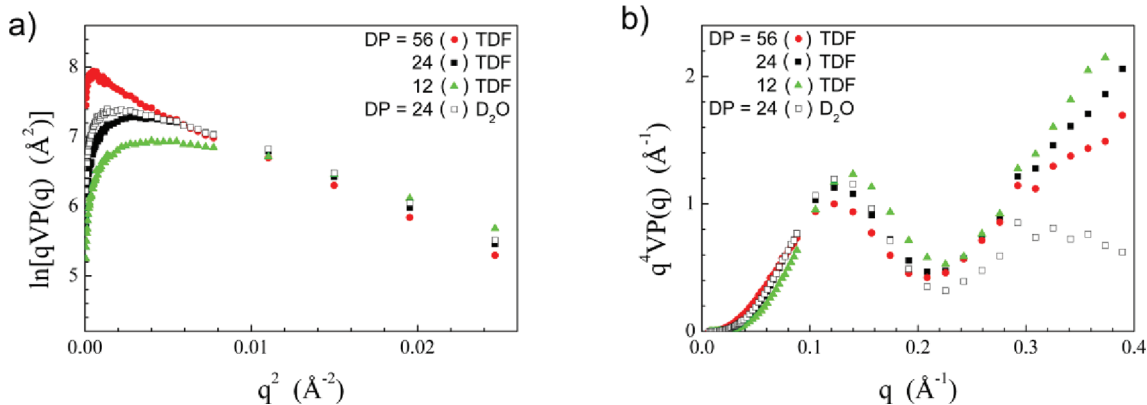


**Figure 13.** Guinier representation of the cylinder cross section (a) and Porod representation of the form factor (b), as determined by SANS from TDF and D<sub>2</sub>O solutions of polymers PG1bis-EO3 as a function of DP.

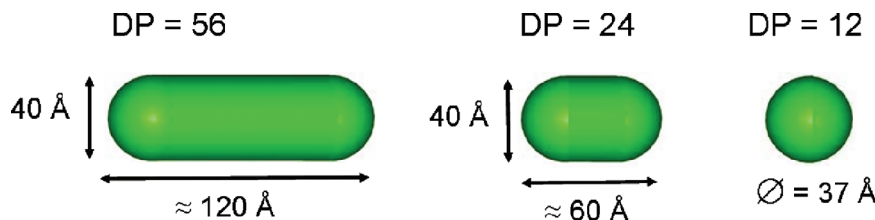


**Figure 14.** Shape evolution of the spherocylinder model for polymers as a function of DP, deduced by SANS studies.

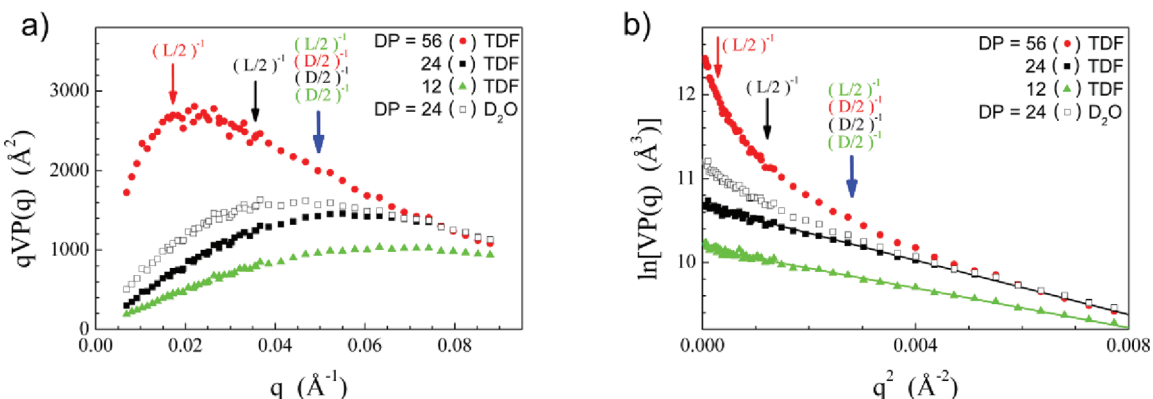


**Figure 15.** Holzer (a) and Guinier (b) representations of the form factors determined by SANS from TDF and D<sub>2</sub>O solutions of polymers PG1bis-EO3 as a function of DP.

from the polydispersity and is explained by the increasing contribution of the overall scattering signal of the high molecular weight polymer fractions. The two other polymers of smaller size (DP = 24 and 12) with lower polydispersities (1.20 and 1.11, respectively) show a linear variation below and even beyond the Guinier range, as expected from the spherocylinder model. The intercepts were consistent with the particle volumes, and gyration radii of about  $R_g = 23$  and 20 Å have been determined for polymers of DP = 24 and 12, respectively. Using the spherocylinder model, we calculated  $R_g$  from experimental polydispersity values using equations from the literature<sup>24</sup> and obtained the same value for polymer of DP = 24 ( $R_g \sim 23$  Å). However, for polymer of DP = 12 (actually reduced to a quasi-spherical morphology) the same calculations led to a smaller value ( $R_g \sim 16$  Å as compared to the experimental value  $R_g = 20$  Å). It is not clear if

the difference has an experimental origin or if it reveals a significant deviation from the model shape.

To conclude with structural properties, calculations<sup>26</sup> have been performed to assess the degree of congestion in our polymers substituted by sterically demanding EO-dendritic side groups. The calculations are based on the experimental spherocylinder diameter value  $d = 40$  Å, assuming that there is a distinct core–shell interface between the polymer inner core and the EO shell. Thus, considering a cylindrical shaped polymer (infinite length), it was calculated that one oligo(EO) chain occupies an average area of about 24 Å<sup>2</sup> at the core–shell interface and that two neighboring monomer units are spaced out of ca. 1.83 Å along the cylinder axis. These results show that the macromolecules are not fully congested since there is still a gap with respect to the lowest limit value of 21 Å<sup>2</sup> for the transverse molecular area of a

"molten" EO chain<sup>26</sup> and of 2.54 Å for the highest distance between two repeat units of a fully stretched (ethylene) polymer backbone. Moreover, this gap toward the fully congested structure is further increased for real polymers of finite length by the presence of tips. Then, using the spherocylinder model and assuming a shell of equal thickness all around the polymer core, the average interface area per EO chain grows to 25, 28, and 32 Å<sup>2</sup> for the EO-dendronized polymers of DP = 56, 24, and 12, respectively. This would confirm that these bis-dendronized polymers PG1bis-EOx are not congested enough and therefore not stiff enough to exhibit mesomorphic properties. The attempt to reach higher degree of congestion with the bulkier tris-dendronized polymers PG1tris-EOx was not successful because the synthesis of the multiallylic precursors (PG1tris) was limited to oligomers of very low DPs.<sup>2h</sup>

## SUMMARY AND CONCLUSION

A series of dendronized polymers carrying short EO peripheral chains have been successfully prepared. The synthesis was performed by thiol–ene coupling of EO chains onto the terminal allyl branches of preformed multiallylic dendronized polymers. Despite the high steric hindrance, the grafting was excellent, leading to a quasi-complete conversion of allyles without any detectable side reaction.

A single and constant glass transition temperature ( $T_g \sim -80^\circ\text{C}$ ) is observed for all EO-containing polymers and macromonomers, indicating that  $T_g$  is solely ruled by the presence of EO chains.

One polymer series having a proper hydrophilic and hydrophobic balance shows a thermoresponsive behavior in water, with the presence of lower critical solution temperatures. Sharp transitions with a narrow hysteresis are observed. Surprisingly, the LCST is found to increase with increasing DP. This uncommon behavior might be explained (in the oligomer regime) by at least two concomitant factors: a polymer dilution effect and an increase of the apparent hydrophilicity of the polymers due to a densification of the EO coverage.

The structural properties of the polymers in solution were investigated by SAXS and SANS. The spherocylinder model gives a quite satisfactory description of the scattering curves for the investigated polymers. More complicated shapes can be envisioned, especially for the tips of the cylinders,<sup>24</sup> but the measurements do not afford the possibility to discriminate between them. Whatever the detail of the model, the results clearly show that the cross section of the scattering objects does not change significantly with the DP, with the solvent type, and in the case of aqueous solutions with the temperature gap prior to the LCST transition. The polymer cross section (40 Å) in solution is comparable to the bulk columnar areas exhibited by analogous mesomorphic dendronized polymers with oligo(dimethylsiloxane) shells, which was shown to be induced by congestion at the core–shell interface and a high degree of polymer backbone stretching.<sup>5</sup>

## ASSOCIATED CONTENT

**Supporting Information.** Synthesis of macromonomers; radical polymerization of the styrene EO-based macromonomer; <sup>1</sup>H and <sup>13</sup>C NMR spectra; SEC traces in water of polymer PG1bis-EO3 of DP = 82. This material is available free of charge via the Internet at <http://pubs.acs.org>.

## AUTHOR INFORMATION

### Corresponding Author

\*E-mail: mery@ipcms.u-strasbg.fr.

### Present Addresses

<sup>†</sup>Institut für Chemie, Technische Universität Berlin, Englische Strasse 20, 10587 Berlin, Germany.

<sup>‡</sup>Department of Chemistry, Institute for Polymer Research, University of Waterloo, 200 University Ave. W., Waterloo, Ontario N2L 3G1, Canada.

## ACKNOWLEDGMENT

Authors are grateful to several collaborators: Dr. A. Rameau from the Institut Charles Sadron (ICS) in Strasbourg for SEC characterizations and related discussions; Dr. E. Ennifar from the Institut de Biologie Moléculaire et Cellulaire (IBMC) in Strasbourg for making possible the turbidimetry measurements; Dr. C. Rochas for technical support for SAXS measurements at the European Synchrotron Radiation Facility (ESRF), Grenoble, France; and Drs. F. Boué and D. Lairez for technical support for SANS measurements at the Laboratoire Léon Brillouin (LLB), CEA-Saclay, France.

## REFERENCES

- (1) Selected reviews in dendronized polymers: (a) Schlüter, A. D.; Rabe, J. P. *Angew. Chem., Int. Ed.* **2000**, *39*, 864–883. (b) Schlüter, A. D. *Top. Curr. Chem.* **2005**, *245*, 151–191. (c) Fraurenath, H. *Prog. Polym. Sci.* **2005**, *30*, 325–384. (d) Rosen, B. M.; Wilson, C. J.; Wilson, D. A.; Peterca, M.; Imam, M. R.; Percec, V. *Chem. Rev.* **2009**, *109*, 6275. (e) Chen, Y.; Xiong, X. *Chem. Commun.* **2010**, *46*, 5049–5060.
- (2) Selected examples of dendronized polymers prepared by the macromonomer strategy: (a) Kaneko, T.; Horie, T.; Asano, M.; Aoki, T.; Oikawa, E. *Macromolecules* **1997**, *30*, 3118–3121. (b) Percec, V.; Ahn, C.-H.; Barboiu, B. *J. Am. Chem. Soc.* **1997**, *119*, 12978–12979. (c) Percec, V.; Schlüter, D. *Macromolecules* **1997**, *30*, 5783–5790. (d) Stocker, W.; Karakaya, B.; Schürmann, B. L.; Rabe, J. P.; Schlüter, A. D. *J. Am. Chem. Soc.* **1998**, *120*, 7691–7695. (e) Zhang, A.; Zhang, B.; Wätersbach, E.; Schmidt, M.; Schlüter, A. D. *Chem.—Eur. J.* **2003**, *9*, 6083–6092. (f) Zhang, A.; Wie, L.; Schlüter, A. D. *Macromol. Rapid Commun.* **2004**, *25*, 799–803. (g) Nyström, A.; Malkoch, M.; Furó, I.; Nyström, D.; Unal, K.; Antoni, P.; Vamvounis, G.; Hawker, C.; Wooley, K.; Malmström, E.; Hult, A. *Macromolecules* **2006**, *39*, 7241–7249. (h) Moingeon, F.; Masson, P.; Méry, S. *Macromolecules* **2007**, *40*, 55–64. (i) Costa, L. I.; Käseme, E.; Storti, G.; Morbidelli, M.; Walde, P.; Schlüter, A. D. *Macromol. Rapid Commun.* **2008**, *29*, 1609–1613.
- (3) Selected examples of preparation of dendronized polymers by a grafting strategy: (a) Ouali, N.; Méry, S.; Skoulios, A. *Macromolecules* **2000**, *33*, 6185. (b) Grayson, S. M.; Fréchet, J. M. J. *J. Am. Chem. Soc.* **2001**, *123*, 6542–6544. (c) Mynar, J. L.; Choi, T.-L.; Yoshida, M.; Kim, V.; Hawker, C. J.; Fréchet, J. M. J. *Chem. Commun.* **2005**, 5169–5171. (d) Guo, Y.; van Beek, J. D.; Zhang, B.; Colussi, M.; Walde, P.; Zhang, A.; Kröger, M.; Halperin, A.; Schlüter, A. D. *J. Am. Chem. Soc.* **2009**, *131*, 11841–11854.
- (4) Selected reports on worm-shaped dendronized polymers: (a) Percec, V.; Ahn, C.-H.; Cho, W.-D.; Jamieson, A. M.; Kim, J.; Leman, T.; Schmidt, M.; Gerle, M.; Möller, M.; Prokhorova, S. A.; Sheiko, S. S.; Cheng, S. Z. D.; Zhang, A.; Ungar, G.; Yeardley, D. J. P. *J. Am. Chem. Soc.* **1998**, *120*, 8619–8631. (b) Förster, S.; Neubert, I.; Schlüter, A. D.; Lindner, P. *Macromolecules* **1999**, *32*, 4043–4049. (c) Yoshida, M.; Fresco, Z. M.; Ohnishi, S.; Fréchet, J. M. J. *Macromolecules* **2005**, *38*, 334–344. (d) Zhang, B.; Wepf, R.; Fischer, K.; Schmidt, M.; Besse, S.; Lindner, P.; King, B. T.; Sigel, R.; Schurtenberger, P.; Talmon, Y.; Ding, Y.; Kröger, M.; Halperin, A.; Schlüter, A. D. *Angew. Chem., Int. Ed.* **2011**, *50*, 737–740. (e) Welch, P. M.; Welch, C. F. *Nano Lett.* **2006**, *6*, 273–277.

- 6, 1922–1927. (f) Efthymiopoulos, P.; Vlahos, C.; Kosmas, M. *Macromolecules* **2009**, *42*, 1362–1369.
- (5) Moingeon, F.; Roeser, J.; Masson, P.; Arnaud, F.; Méry, S. *Chem. Commun.* **2008**, *11*, 1341–1343.
- (6) (a) Kim, C.; Kang, S. *J. Polym. Sci., Part A: Polym. Chem.* **2000**, *38*, 724–729. (b) Kim, C.; Kwark, K. *J. Polym. Sci., Part A: Polym. Chem.* **2002**, *40*, 976–982.
- (7) (a) Li, W.; Zhang, A.; Schlüter, A. D. *Macromolecules* **2008**, *41*, 43–49. (b) Li, W.; Zhang, A.; Schlüter, A. D. *Chem. Commun.* **2008**, 5523–5525. (c) Li, W.; Zhang, A.; Feldman, K.; Walde, P.; Schlüter, A. D. *Macromolecules* **2008**, *41*, 3659–3667. (d) Li, W.; Schlüter, A. D.; Zhang, A. *J. Polym. Sci., Part A: Polym. Chem.* **2009**, *47*, 6630–6640. (e) Bolisetti, S.; Schneider, C.; Polzer, F.; Ballauff, M.; Li, W.; Zhang, A.; Schlüter, A. D. *Macromolecules* **2009**, *42*, 7122–7128. (f) Junk, M. J. N.; Li, W.; Schlüter, A. D.; Wegner, G.; Spiess, H. W.; Zhang, A.; Hinderberger, D. *Angew. Chem., Int. Ed.* **2010**, *49*, 5683–5687.
- (8) Lapienis, G. *Prog. Polym. Sci.* **2009**, *34*, 852–892 and references therein.
- (9) (a) Masson, P.; Beinert, G.; Franta, E.; Rempp, P. *Polym. Bull.* **1982**, *7*, 17–22. (b) Ito, K.; Tomi, Y.; Kawaguchi, S. *Macromolecules* **1992**, *25*, 1534–1538. (c) Lahitte, P. J.; Pelascini, F.; Peruch, F.; Plentz Meneghetti, S.; Lutz, P. J. *C. R. Chim.* **2002**, *5*, 225–234. (d) Lutz, J. F. *J. Polym. Sci., Part A: Polym. Chem.* **2008**, *46*, 3459–3470.
- (10) (a) Bo, Z.; Rabe, J. P.; Schlüter, A. D. *Angew. Chem., Int. Ed.* **1999**, *38*, 2370–2372. (b) Bo, Z. B.; Zhang, C.; Severin, N.; Rabe, J. R.; Schlüter, A. D. *Macromolecules* **2000**, *33*, 2688–2694. (c) Yi, Z.; Liu, X.; Jiao, Q.; Chen, E.; Chen, Y.; Xi, F. *J. Polym. Sci., Part A: Polym. Chem.* **2008**, *46*, 4205–4217.
- (11) (a) Nabeshima, T.; Takahashi, T.; Hanami, T.; Kikuchi, A.; Kawabe, T.; Yano, Y. *J. Org. Chem.* **1998**, *63*, 3802–3803. (b) Snow, A.; Foos, E. *Synthesis* **2003**, 509–512.
- (12) Lorenz, K.; Frey, H.; Stühn, B.; Mühlaupt, R. *Macromolecules* **1997**, *30*, 6860–6868.
- (13) Justynska, J.; Hordyjewicz, Z.; Schlaad, H. *Polymer* **2005**, *46* (26), 12057–12064.
- (14) Gil, E. S.; Hudson, S. M. *Prog. Polym. Sci.* **2004**, *29*, 1173–1222.
- (15) (a) Wei, H.; Chen, S.-X.; Zhang, X.-Z.; Zhuo, R.-X. *Prog. Polym. Sci.* **2009**, *34*, 893–910. (b) Liu, R.; Fraylich, M.; Saunders, B. R. *Colloid Polym. Sci.* **2009**, *287*, 627–643. (c) Klouda, L.; Mikos, A. G. *Eur. J. Pharm. Biopharm.* **2008**, *68*, 34–45. (d) Mano, J. F. *Adv. Eng. Mater.* **2008**, *10*, S15–S27.
- (16) Schild, H. G. *Prog. Polym. Sci.* **1992**, *17*, 163–249.
- (17) (a) Aoshima, S.; Oda, H.; Kobayashi, E. *J. Polym. Sci., Part A: Polym. Chem.* **1992**, *30*, 2407–2413. (b) Han, S. H.; Hagiwara, M.; Ishizone, T. *Macromolecules* **2003**, *36*, 8312–8319. (c) Lutz, J.-F.; Akdemir, Ö.; Hoth, A. *J. Am. Chem. Soc.* **2006**, *128*, 13046–13047. (d) Hua, F.; Jiang, X.; Li, D.; Zhao, B. *J. Polym. Sci., Part A: Polym. Chem.* **2006**, *44*, 2454–2467.
- (18) (a) Li, W.; Zhang, A.; Chen, Y.; Feldman, K.; Wu, H.; Schlüter, A. D. *Chem. Commun.* **2008**, 5948–5950.
- (19) (a) Haba, Y.; Harada, A.; Takagishi, T.; Kono, K. *J. Am. Chem. Soc.* **2004**, *126*, 12760–12761. (b) Haba, Y.; Kojima, C.; Harada, A.; Kono, K. *Angew. Chem., Int. Ed.* **2007**, *46*, 234–237.
- (20) (a) Hietala, S.; Nyström, A.; Tenhu, H.; Hult, A. *J. Polym. Sci., Part A: Polym. Chem.* **2006**, *44*, 3674–3683. (b) Gao, M.; Jia, X.; Kuang, G.; Li, Y.; Liang, D.; Wei, Y. *Macromolecules* **2009**, *42*, 4273. (c) Gao, M.; Jia, X.; Li, Y.; Liang, D.; Wei, Y. *Macromolecules* **2010**, *43*, 4314.
- (21) Xia, Y.; Yin, X.; Burke, A. D.; Stöver, H. D. H. *Macromolecules* **2005**, *38*, 5937–5943.
- (22) Alami, E.; Rawiso, M.; Isel, F.; Beinert, G.; Binana-Limbele, W.; François, J. *Adv. Chem. Ser.* **1996**, *248*, 343–362.
- (23) Kujawa, P.; Segui, F.; Shaban, S.; Diab, C.; Okada, Y.; Tanaka, F.; Winnik, F. M. *Macromolecules* **2006**, *39*, 341–348.
- (24) (a) Kaya, H.; de Souza, N. R. *J. Appl. Crystallogr.* **2004**, *37*, 508. (b) Kaya, H. *J. Appl. Crystallogr.* **2004**, *37*, 223.
- (25) See for instance: Schmidt, R.; Schmutz, M.; Mathis, M.; Decher, G.; Rawiso, M.; Mésini, P. *Langmuir* **2002**, *18*, 7167.
- (26) The calculations were performed from partial volumes determined by dilatometric measurements and as described in ref 5.